

COVER PAGE

Document downloaded by @DAEL

Fri Nov 27 16:10:50 2026
For personal use

When automatic English translation is provided, only the original document is authentic.
The EAA cannot be held responsible of any translation error

Bibliographical reference

An Improved Correction Method for Sound Source Drift in A Jet Flow and Its Application to A Wind Tunnel Measurement, Yigang Wang, Jiashun Yang, Qing Jia, Zhigang Yang and Zhe Shen, Acta Acustica **vol. 101** (Number 3), 2015, pp. 642-649

DOI
https://doi.org/10.3813/AAA.918859

Acta Acustica united with Acustica
Vol. 101 (2015) 642 – 649

Technical and Applied Papers
DOI 10.3813/AAA.918859

An Improved Correction Method for Sound Source Drift in A Jet Flow and Its Application to A Wind Tunnel Measurement

Yigang Wang, Jiashun Yang, Qing Jia, Zhigang Yang, Zhe Shen
Shanghai Automotive Wind Tunnel Center, Tongji University, 201804, Shanghai, China.
yigang.wang@sawtc. com

Summary
The change of sound propagation characteristics during sound propagation in jet flow in an open-jet wind tunnel makes the sound information distorted, which is obtained from outside of the jet flow. This paper focuses on the variation of sound propagation direction, which is one of main features for the change of sound propagation. On the basis of the average flow pattern in the shear layer of jet flow which is obtained by CFD method, the simplified shear layer flow model is put forward. By combining the flow model with the geometrical acoustics theory, an improved correction method is presented to estimate the drift of sound source position of a point source in the core area caused by sound propagation in jet flow. Furthermore, the sound source drifts due to variation of sound propagation direction in jet flow of an aero-acoustic wind tunnel were calculated by CFD method. At the mean time they were tested in the same aero-acoustic wind tunnel. Compared to results from the test and Amiet's method, more precise calculation results regarding sound source drift at different sound source positions along the jet flow direction can be obtained via the improved correction method in this paper. The improved correction method can be applied not only to correct the results measured from the outside of jet flow in a wind tunnel test, but also to analyze the sound propagation process in the jet flow.

PACS no. 43.20.-f

1. Introduction

Jet flow exists in many circumstances, such as an airplane engine jet and a jet flow in an open-jet wind tunnel. Studies [1, 2, 3, 4, 5, 6, 7, 8, 9, 10] show that jet flow can seriously affect the sound propagation from inner sound source to external space, including changes of sound propagation path, variation of signal strength and broadening of tone, etc, which will result in inaccurate observation outside the jet flow. For example, in an open-jet aero-acoustic wind tunnel test, the sound source information cannot be measured accurately outside the shear layer because of the change of sound propagation due to jet flow. It is always difficult to get a satisfied solution due to the unsteady characteristics of jet flow and complicated sound propagation pattern in flow.

The researches on the sound propagation of jet flow emphasized on the shear layer. The earliest studies were aimed to predict aircraft jet noise [1, 5, 8, 9]. The theory to estimate the noise of aircraft [11] is complicated due to refraction in the shear layer between the turbulent jet and the ambient medium, which has been the subject of various attempts in theoretical modeling for more than a decade (e.g. [12, 13]. Their studies showed that the refraction may be caused by parts of the Lighthill stress tensor in a complex flow. In all researches mentioned above, the refraction has been considered as a sound source effect, rather than a sound propagation effect, which is not consistent with the actual situation. Lilley [14] has simplified the complex flow as a parallel movement and average flow, and derived a differential equation to describe the refraction in a shear layer by differentiating sound source and sound propagation. However, it was difficult to get solutions [15, 16]. As a result, it was rarely put into practice. Amiet studied the effect of refraction based on the theory of plane wave sound propagation between two flows via relative motion and geometric acoustics [2, 3]. Then Candel [4], Plumblee [17], Amiet [6], Schlinker [7] and Ahuja [8] developed Amiet's method [3, 5, 6, 8, 9]. They modeled the shear layer as an infinitely thin cylindrical vortex sheet, where the jet flow and the ambient were assumed to be homogeneous. But the simulation of shear layer was too simple to reflect the comprehensive properties of jet flow, which introduced a relatively large deviation [8]. It was difficult to obtain results conforming to the reality. However, Amiet's method has been applied in certain cases [18, 19, 20, 21].

In this paper, based on the fact of shear layer that both the thickness along the flow direction and the internal velocity distribution have changed, the sound propagation

Received 08 October 2013,
accepted 10 December 2014.

© S. Hirzel Verlag · EAA

model in a wind tunnel jet flow and the prediction method of sound propagation path are studied in combination with the methods of aero-acoustic wind tunnel test, numerical simulation and geometrical acoustics theoretical analysis. And then, this method is used to calculate the sound source drifts caused by the variation of sound propagation direction in jet flow inside an aero-acoustic wind tunnel. Accordingly, the sound source drifts are tested in the same aero-acoustic wind tunnel. Compared with the test results and Amiet's method, the advantages and applicability of the method in this paper will be further indicated.

2. Numerical simulation analysis of jet flow

The study in the paper aims to predict the influence of jet flow on sound propagation by the geometric acoustic method. To thoroughly avoid the defects of simplified model of shear layer in Amiet's method, the characteristics of the shear layer were firstly studied by CFD method. Based on numerical simulating results, a sound propagation model was presented. Then the method of predicting sound propagation path was developed.

2.1. Simulating model, mesh and boundary condition

A numerical model of a full scale aero-acoustic wind tunnel was established, with a test section size of 21 m × 17 m × 12 m, and the nozzle size of 6.5 m × 4.25 m. To avoid of inverse flow, an extended section was added behind the diffuser, as shown in Figure 1. The computation domain was divided by hexahedral grid by an ICEM commercial code, as shown in Figure 2. The thickness of first prism layer for the wall inside the test section is 5 mm with a growth ratio of 1.2 along the normal direction. The thickness of boundary layer at test section wall is 12 mm. The mesh in the shear layer area was refined. The mesh size near the wall of the nozzle is 10 mm. And the biggest mesh size along the flow direction is 25 mm. The size of mesh perpendicular to the flow direction is 30–40 mm. The total number of grids is 4.12 million. The commercial code FLUENT was used as the solver in this paper. Details about boundary condition setting are shown in Table I. The turbulence intensity of the inlet was acquired through results of the aero acoustic wind tunnel test.

The inlet velocities are equal to the velocities of the jet flow potential core in the wind tunnel test: 120 km/h, 140 km/h, 160 km/h, 180 km/h, 200 km/h, 210 km/h, 220 km/h, 230 km/h, 240 km/h and 250 km/h. Because of the complexity of transient features in a shear layer, only the steady flow was simulated to get the mean characteristics of the flow field.

2.2. Validity of the numerical results

In order to validate the numerical results, some experimental verification were carried out in a wind tunnel. The wind tunnel is the same as the wind tunnel used in the above numerical simulation analysis. The pressure coefficient (Cp)

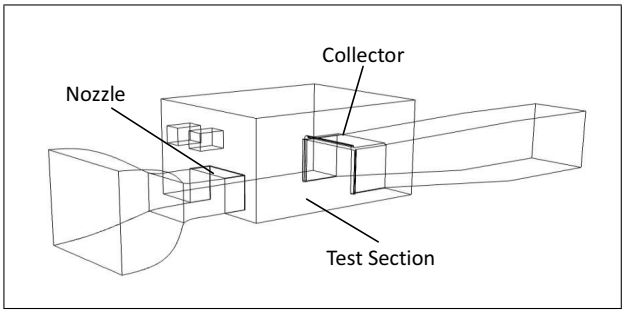

Figure 1. Schematic plot of numerical domain.

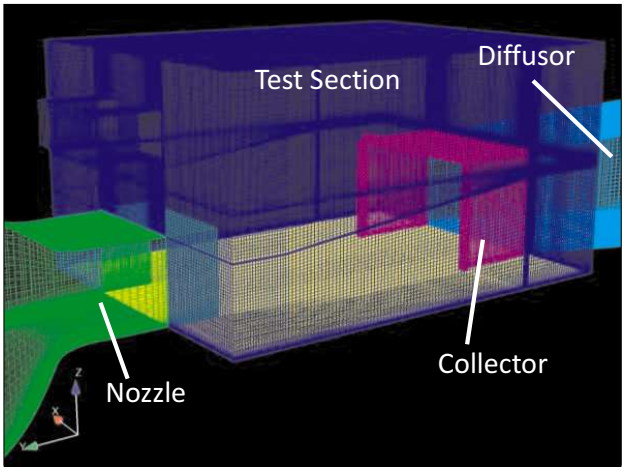

Figure 2. Meshes in numerical domain.

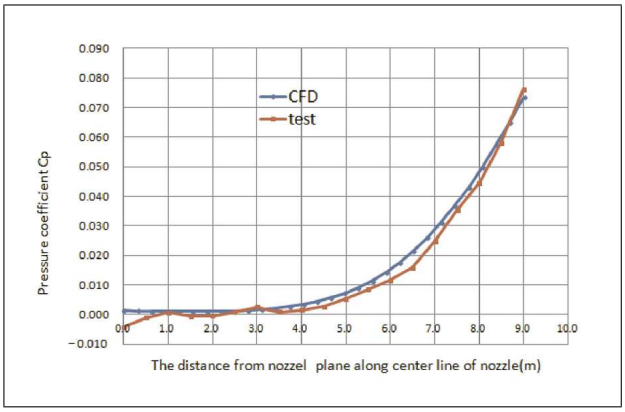

Figure 3. The pressure coefficient compare between the CFD and the test.

figure along the center line of nozzle outlet plane, which is 0.6 m high away from the floor, was measured. The Cp figure for same line was obtained by CFD method at the same time. The numerical estimation shows good agreement with the experiment result, as shown in Figure 3.

2.3. Mean velocity distribution of jet flow

The case with nozzle outlet plane flow speed of 140 km/h is taken as an example to investigate the characteristics of mean velocity in a jet flow. The velocity gradient in a shear layer has great impact on sound propagation. Therefore, it is necessary to analyze velocity features. Figure 4 and

Table I. FLUENT simulation setting.

Solver	Separated
Turbulence model	Realizable
Boundary foundation	Un-balanced
Velocity inlet	Turbulence intensity: 1% (from test) Turbulence viscosity: 10
Outlet	Outflow
Inlet vent	Inlet-vent

Figure 5 show the velocity contours of the jet flow at a plane of 800 mm high above the floor and at the symmetry plane along the flow direction respectively.

Due to restriction of the walls and the effect of collectors in the test section, the jet flow belongs to finite-space type flow. Figure 4 and Figure 5 show that only those test section walls near to the collectors can affect the expansion of the shear layer in a jet flow. So the jet flow both above and beside the nozzle, with a long distance to the collectors, can be treated as free jet flow approximately. As a result, the flow velocity in the direction of central line remains constant, which forms the jet potential core area. The flow outside the jet core area has a relatively low speed, and its impact on sound propagation can be ignored. So air in this area is considered as being stationary. The part between two areas mentioned above contains the shear layer with a velocity gradient. Thickness of the shear layer increases along the flow direction.

2.4. Velocity distribution in the shear layer

As shown in Figure 4 and Figure 5, the velocity decreases in the transverse direction from the inner boundary to the outer boundary of shear layer, which induces a velocity gradient. Moreover, the shear layer area is gradually extended along the jet flow direction. Both velocity gradient and shear layer extension affect the sound propagation in transverse and longitudinal directions of the shear layer. Thus the current simplified method (Amiet's method) considering the shear layer as a vortex shell is obviously not reliable and has large deviation from what actually happens. On the plane of 800 mm high above floor, Figure 6 shows the shear layer velocity distribution in the transverse direction at different distances away from the nozzle at a speed of 140 km/h. From Figure 6, it is learned that the velocity decreases from the potential core to outer area of the shear layer in different laws. The velocity distribution is nonlinear at the region between the potential core and the shear layer, as well as the region between the shear layer and the stationary air area. However, the velocity distribution is approximately linear in the shear layer. Along the jet flow direction, the thickness of shear layer increases, the velocity distribution varies and the velocity gradient decreases.

In order to briefly outline the velocity distribution in the shear layer, take the jet flow at speed of 140 km/h as an

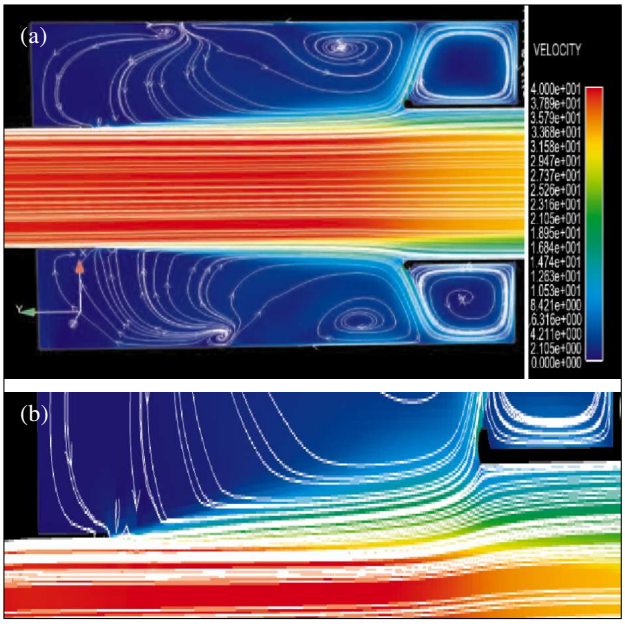

Figure 4. Velocity path line contour on horizontal cross section of $z = 800$ mm. (a) Velocity path line contour of the test section, (b) Velocity path line contour of the shear layer.

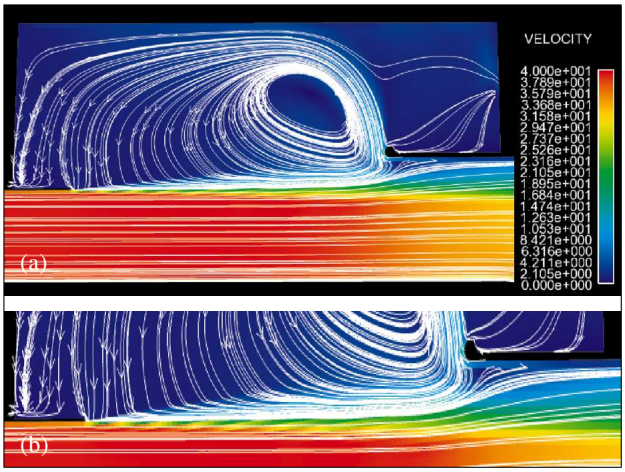

Figure 5. Velocity path line contour on axle symmetry plane. (a) Velocity path line contour of the test section, (b) Velocity path line contour of the shear layer.

example. The transverse shear layer velocity distribution at a height of 800 mm above the floor and a distance of 7000 mm away from the nozzle is linearly fitted as shown in Figure 7, where $U = 0.003y + 39.53$ represents the velocity in the potential core area, $U = 0.038y + 1.622$ expresses the velocity in stationary air area and $U = -27.27y + 112.9$ displays the velocity in shear layer area, the maximum deviation is about 10%. x is the stream wise direction and y is the transverse direction.

Similarly, the thickness variation of shear layer can be obtained by fitting both boundaries of the shear layer as slant lines, which are shown in Figure 8. The formula for the outer linear fitting is $U = 0.053y + 3.390$, the maximum deviation is about 2%, and that for the inner is $U = -0.028y + 3.108$, and the maximum deviation is about 1%.

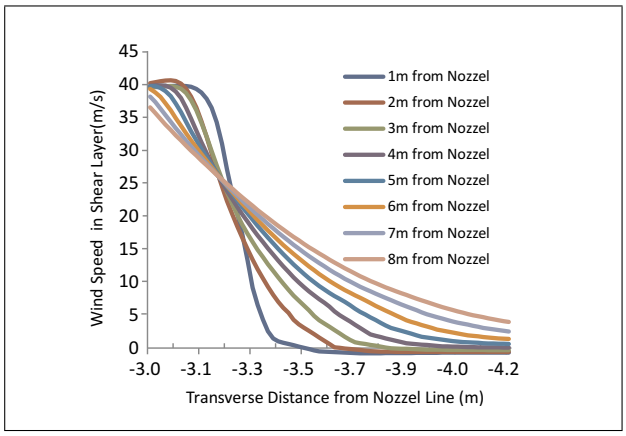

Figure 6. Shear layer velocity distribution on the transverse direction with different distance from nozzle high above floor 800 mm.

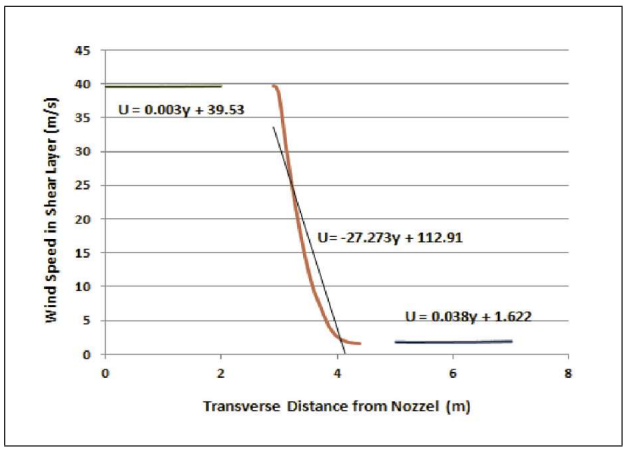

Figure 7. Velocity distribution fitting figure at height of 800 mm (wind speed of the nozzle is 140 km/h).

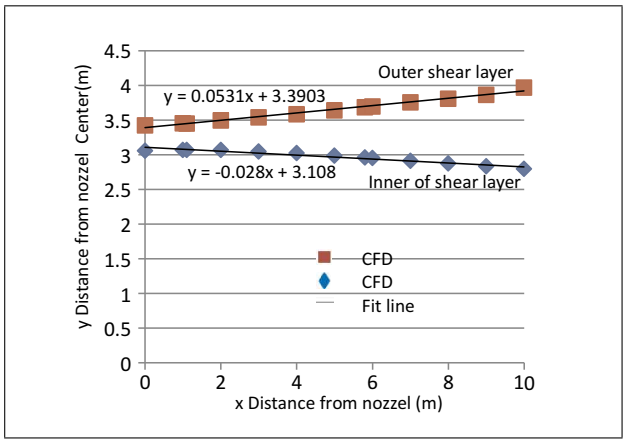

Figure 8. The thickness of the shear layer along the jet flow direction (wind speed of the nozzle is 140 km/h).

3. Sound propagation calculation in jet flow

Sound propagation in jet flow is closely related to the flow of shear layer, especially the velocity distribution. As showed by the above flow analysis, the thickness varies both in the transverse direction and in the jet flow direction, and the velocity gradient of shear layer also appears both in the transverse direction and in the jet flow direction. Obviously, it is a highly simplified assumption to consider the shear layer as a vortex shell in Amiet's method. Based on the numerical simulating results, the sound source drift during the sound propagation in shear layer can be deduced as follows.

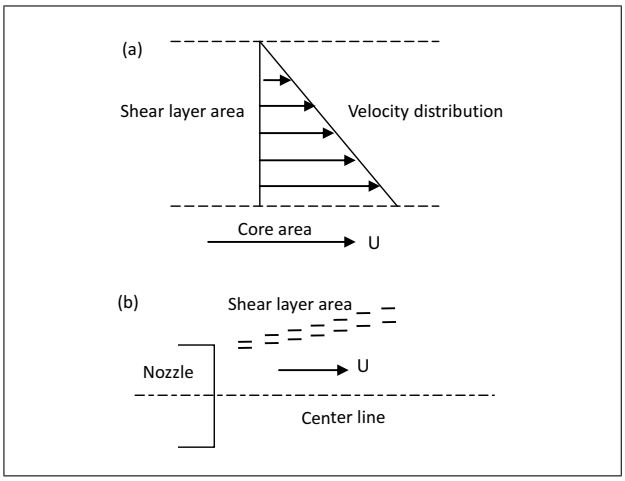

Figure 9. Simplified model for shear layer. (a) Velocity distribution in shear layer (b) Discretization for shear layer.

3.1. Hypothetical models

The jet flow potential core is supposed to be an uniform flow area, the flow outside the shear layer is stationary and the transverse velocity distribution in shear layer is linear, as shown in Figure 9a, determined by the numerical simulation mentioned above. The thickness of shear layer also increases linearly along the jet flow direction, also determined by the numerical simulation. To simplify the calculation, both inner and outer boundary lines of the shear layer are supposed to be numerous short parallel lines, as shown in Figure 9b. A point sound source is supposed to be at the center line of the potential core area. Figure 10 shows how the source propagates in a jet flow.

3.2. Sound source drift calculation

As shown in Figure 10, θ' and R' represent respectively the radiation angle and the propagation path of sound waves in stationary air. As the air flow goes downstream, the sound wave actually propagates along path R with the angle θ when it propagates in straight lines in the potential core area and the stationary air area. In the shear layer area, the sound propagation path changes based on the above hypothesis. By the geometrical relationship the following equation is derived:

$$R_m \cos\theta_m = R_t \cot\theta + \frac{(0.5U - c_0\cos\theta')s}{c_0 \sin\theta'} + \left(R_m \sin\theta_m - R_t - s\right)\cos\theta_0, \quad (1)$$

where, R_m is the distance between the observation point and the sound source. R_t is the distance between the cen-

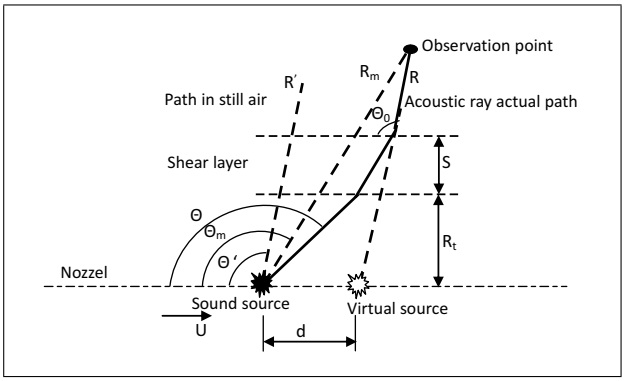

Figure 10. Sound propagation model in jet flow.

ter line of nozzle and inner boundary of shear layer. θ is the angle between the actual propagation path in jet flow potential core and the centerline of nozzle. U is velocity in the potential core. c_0 is sound velocity. s is local shear layer thickness. θ_m is angle between the centerline of nozzle and the line connecting the sound source with the observation point. θ_0 is angle between the propagation path in stationary air and the centerline of nozzle. θ' is angle between the sound propagation path and the centerline of nozzle in the case of without jet flow and jet flow velocity is zero. Here in the equation $\theta' = \theta_0$. M is Mach number of the jet flow.

According to the convection effect of geometrical acoustic method, the following equation is obtained:

$$\theta' = \cos^{-1}\left[M\sin^2\theta + \cos\theta\sqrt{1 - M^2\sin^2\theta}\right]. \tag{2}$$

In the flow, the velocity of sound wave along the shear layer is determined by the flow velocity U and the sound velocity in the flow C_t. Velocity along jet flow direction in shear layer is signed as U_{tr}. According to Snell's law [9], U_{tr} can be calculated as

$$U_{tr} = U - \frac{c_t}{\cos\theta'} = \frac{-c_0}{\cos\theta_0}, \tag{3}$$

$$M = \frac{U}{c_t} = \frac{1}{\cos\theta'} - \frac{c_0/c_t}{\cos\theta_0}. \tag{4}$$

According to the geometrical relationship displayed in the Figure 10, the sound source drift d is the distance between the virtual sound source and the actual sound source, which is as

$$d = R_m \sin\left(\theta_m - \theta_0\right) \Big/ \sin\theta_0. \tag{5}$$

On the basis of Equations (1) to (4), the angle parameters needed in Equation (5) can be obtained.

4. Measurement of sound source drift in an aero-acoustic wind tunnel

4.1. Test platform

Measurements were conducted in a 3/4 open-jet aero-acoustic wind tunnel, a rectangular nozzle with an exit

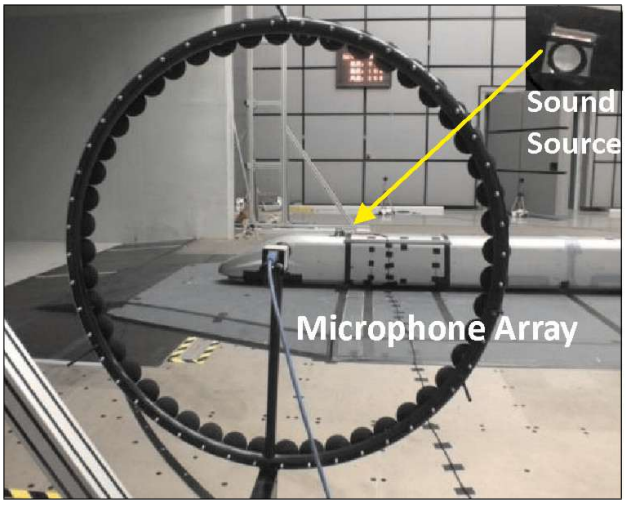

Figure 11. Position of sound source and test facilities in wind tunnel test section.

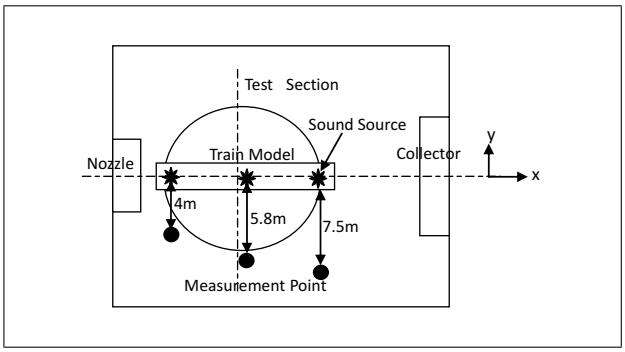

Figure 12. Position of sound source and microphone array.

area of 27 m^2. The wind tunnel is the same as what is used in the numerical simulation analysis, namely a rectangular nozzle with the outlet dimension of 6.5 m×4.25 m and the turbulence intensity of 1%. As shown in Figure 11 and Figure 12, speakers were mounted on a 1:8 scaled high-speed train model, which is placed on the floor of the test section along the centerline of the nozzle. The train model is a three-car model, with its length at 9.74 m, height at 0.51 m and width at 0.43 m. The surface and the bottom of the train model were smoothed to ensure lower background noise level. Speakers generated white noise at the head section, the middle section and the tail section of the train respectively. A 48-channel microphone array manufactured by Gfai Company in Germany was placed outside the flow field as a receiver, while the deconvolution beamforming algorithms and the high dynamic range algorithm [22, 23] were adopted. The array is a microphone array ring. The diameter is 1.0 meter. 1/4 free field microphones were distributed on the circumference of the ring array. The array system dynamic range is 6–20 dB. The sampling rate is 192 kHz and the sampling time is 8 seconds. Resolution (streamwise direction) was 150 pixels. The FFT was performed on the complete time signal. Block size was 4096. Window function was Von Hann and the overlap 1 frame. They were in default setting in the Gfai software.

The smaller the distance from the microphone array to the sound source the better effect it could be obtained. But because of the jet flow, the microphone array should be set out of the flow. So the microphone array was positioned 4 m, 5.8 m and 7.5 m respectively far away from the head, the middle and the tail.

By measuring the positions of the sound sources with wind and without wind, the effects of jet flow on sound propagation could be identified clearly.

4.2. Influence of boundary layer on sound propagation

Because of the influence of jet flow, speakers should be installed appropriately to avoid strong aerodynamic noise. In order to get lower background noise and to improve the signal-to-noise ratio, a train model was adopted to support the speakers. It is convenient to install the speaker on the surface of the train model at different positions along the stream wise direction. However, a boundary layer around the model would be generated and that would affect the sound propagation. For this sake, the thicknesses of the boundary layer on the surface of the train model at different positions and wind speeds were estimated by the equation (6) before the acoustic experiment was conducted.

$$\delta = 0.37\left(\frac{\nu}{U}\right)^{1/5} x^{4/5}, \tag{6}$$

where δ is the thickness of the boundary layer, ν the kinematic viscosity coefficient, x is the distance from the stagnation point of the head of the train to the observation point.

The thicknesses of the boundary layer on the surface are 8 mm–20 mm at the head section, 50 mm–57 mm at the middle section and 90 m–100 mm at the tail section respectively at wind speeds of 120 km/h–250 km/h, as shown in Figure 13. According to the estimated results, a 70 m height of the sound center was determined to install speakers in the experiments, as shown in Figure 11 and Figure 14a. It is obvious that the thicknesses of the boundary layer on the surface of the head and the middle of the train are smaller than the height of the sound center, so that sound propagates outside the boundary layer and the influence of the boundary layer on the test results is minor. But at the tail of the train, the sound center is in the boundary layer affecting the sound propagation. The test results from speakers on the head and the middle of the train are able to reflect the sound propagation in the shear layer of the jet flow, while the test result from the speaker on the tail of the train is for reference only.

4.3. Sound source drift measurement

The direction of sound propagation changed due to wind speed in the potential core of the jet flow and the refraction by the shear layer during the sound propagation in jet flow. The microphone array was used to locate the sound source in both cases with or without jet flow. The variation of position is described as sound

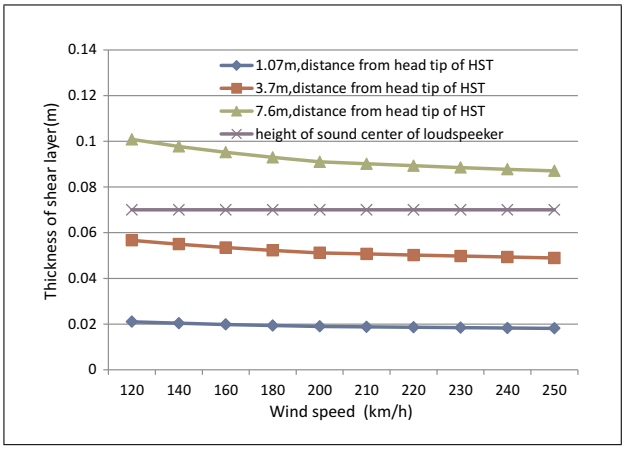

Figure 13. Thicknesses of the boundary layer and height of sound center.

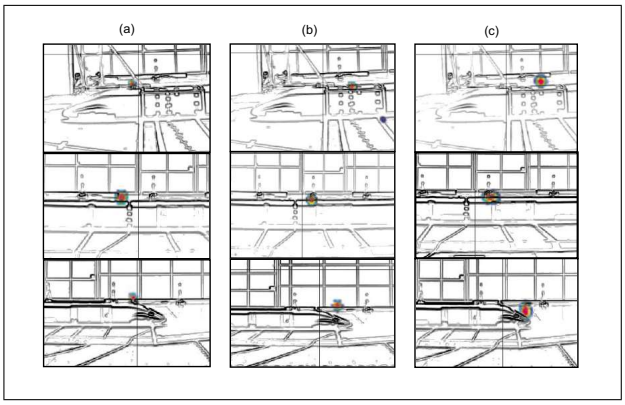

Figure 14. Test result of sound source drift. (a) Position of sound source at zero speed, (b) Position of sound source at 200 km/h speed, (c) Position of sound source at 2.

source drift. The wind speeds from the nozzle were set to120 km/h, 140 km/h, 160 km/h, 180 km/h, 200km/h, 210 km/h, 220 km/h, 230 km/h, 240 km/h and 250 km/h respectively. Figure 14 shows the positions of three sound sources at the head, the middle, and the tail of the train measured by the microphone array are at the speed of 0 km/h, 200 km/h and 250 km/h respectively. Their differences were the values of the sound source drift at the speed of 200 km/h and 250 km/h respectively. Other sound source drifts at different wind speeds and different sections of the model were shown in Figure 15.

As shown in Figure 15, the drift increases dramatically with wind speed. The differences between the drift of sound source at the head and that at the middle section of the train are small and the drift at the head is slightly larger. But the difference between the drifts at the tail and at the head is more significant, with the drift value at the tail being smaller. Sound source drift fluctuates with wind speed at the tail section, which is perhaps caused by the disturbance of the boundary layer on the train. Two factors are considered to contribute to this result. One is that the jet flow near the nozzle is relatively steady, where the shear layer is thinner and the velocity gradient is larger, causing more refraction on sound propagation. With sufficient

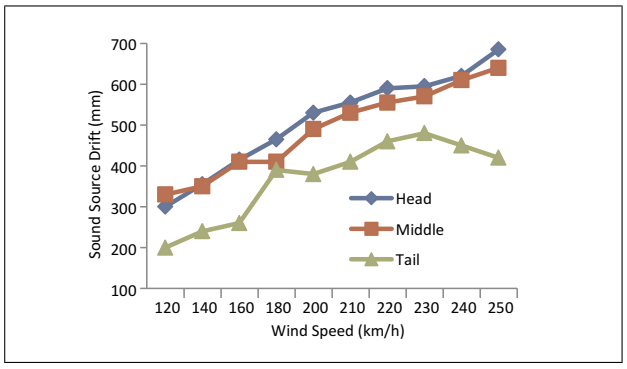

Figure 15. Variation of sound source shift with different wind speed and sound source position.

mixture of jet flow and stationary air around it, the shear layer thickness is enlarged along the flow direction. Meanwhile, the velocity gradient along the transverse direction is decreased. As a result, the refraction on sound propagation is weakened, which makes the sound source drift decrease. Equations (1) and (5) also show that the smaller thickness of the shear layer S is the larger the source drift d will be. So both the shear layer thickness and the velocity gradient affect the source drift. The other factor comes from the high speed train model itself, which acts as the sound source mounting bracket. Boundary layer will appear and grow around the train model at positions of the middle section and the tail section, where the flow separation will occur at the same time. Both factors, together with the shear layer, play a role on the large fluctuation of drift changing with wind speed. The test results show that when the test of an aerodynamic noise source identification for a model is carried out in an aero-acoustic wind tunnel, especially with a long test object and a number of noise sources, the sound source drift at different positions will be affected by both the jet flow and the flow field around the object which are caused by the object itself.

4.4. Comparison of sound source drifts by using different methods

Results from the method presented in this paper and the Amiet's method are compared to the measurement data. The jet flow speeds are set to 120 km/h, 140 km/h, 160 km/h, 180 km/h, 200 km/h, 210 km/h, 220 km/h, 230 km/h, 240 km/h and 250 km/h, respectively. Figure 16 displays the sound source drift with jet flow velocity in the case of different sound source positions, i.e. at the head section, the middle section and the tail section of the train model.

Figure 16 shows that the sound source drift value from the method presented in this paper matches very well with the test results. The deviation was about 2% when the source was at the position of head section, 3% at the position of middle section and 9% at tail section. Nevertheless, the deviation results from Amiet's method are about 2%, 6% and 42% respectively. The error is relatively larger when the source is at the position of tail section. The major reason lies in that the center of sound source (the height of

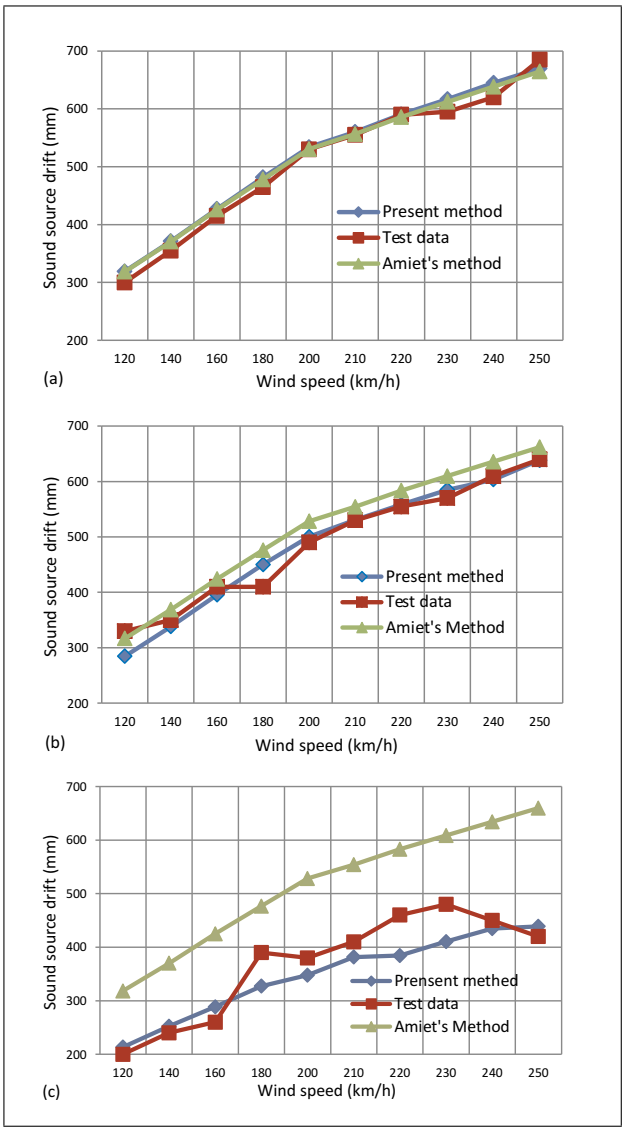

Figure 16. Drift comparison for different methods. (a) Sound source at head of high speed train model (b) Sound source at middle of high speed train model (c) Sound source at tail of high speed train model.

the center is 70 mm) was submerged in the boundary layer around the tail section (the thickness of the boundary layer is 90 mm–100 mm), and the boundary layer disturbed the direction of the sound propagation. This was not considered in the present method and a big error is acceptable. Thus the prediction with the present method proposed in the paper can precisely calculate the sound source drift at different sound source positions. But the Amiet's method is only suitable to confirm the sound source drift near the nozzle. The comparison indicates that the sound propagation in shear layer is related to the velocity gradient in shear layer and with the thickness of the shear layer more apparently.

5. Conclusion

An improved correction method for sound source drift in a jet flow and its application to a wind tunnel measure-

ment are conducted in the paper. To overcome the limitation of Amiet's method, the CFD method is used to analyze the flow features in the shear layer of jet flow. By numerical simulation, the transverse velocity distribution and the shear layer variation law along jet flow direction are obtained. Based on these results, the relationship between velocity variations in shear layer and the change on thickness changes of shear layer are obtained by the linear fitting method. Then a simplified flow model in the shear layer is put forward.

According to the geometrical acoustic theory and the simplified flow model in the shear layer, an improved correction method is presented to estimate the sound source drift when the sound propagates from the center line of the potential core to receivers outside the jet flow. And then, the method is used to calculate the sound source drifts caused by the jet flow in an aero-acoustic wind tunnel. Accordingly, the sound source drifts are measured in the same aero-acoustic wind tunnel. A comparison of the improved correction method to the Amiet's method and the test in the aero-acoustic wind tunnel shows that the improved correction method can be used to estimate the sound source drift in different sound source positions more precisely. The improved correction method can be used to analyze the sound propagation in jet flow. It can also be applied to correct the measurement results from the outside of the jet flow in a wind tunnel test.

Acknowledgement

This project is supported by National Natural Science Foundation of China (Grant No. 51375342).

References

[1] L. M. B. C. Campos: The spectral broadening of sound by turbulent shear layers. Part 2: The spectral broadening of sound and aircraft noise. J. Fluid Mech. **89** (1978) 761–783.

[2] R. Ross: Spectral broadening effects in open wind tunnel in relation to noise assessment. AIAA Journal **19** (1981) 567–572.

[3] R. K. Amiet: Correction of open jet wind tunnel measurements for shear layer refraction. American Institute of Aeronautics and Astronautics, Aero-Acoustics Conference, 2nd, Hampton, Va., Mar. 24-26, 11, 1975.

[4] S. Candel, A. Guedel, A. Julienne: Refraction and scattering of sound in an open wind tunnel flow. Proceedings of the sixth international congress on instrumentation in aerospace simulation facilities, 1975, Vol. 5, 288–300.

[5] T. F. Balsa: Refraction and shielding of sound from a source in a jet. J. Fluid Mech. **76** (1976) 443–456.

[6] R. K. Amiet: Refraction of sound by a shear layer. Journal of Sound and Vibration **58** (1978) 467–482.

[7] R. H. Schlinke, R. K. Amiet: Refraction and scattering of sound by a shear layer. 6th AIAA Aeroacoustics Conference, Hartford, Ct, June 4-6, 1980, AIAA Paper 80–0973.

[8] K. K. Ahuja, H. K. Tanna, B. J. Tester: An experimental study of transmission, refraction and scattering of sound in a free jet flight simulation facility and comparison with theory. Journal of sound and vibration **75** (1981) 51–85.

[9] J. T. Mueller: Aero acoustic measurement. Springer, 2002.

[10] Z. Sulaiman: Effect of open-jet shear layers on aero acoustic wind tunnel measurements. For obtaining the degree of Master of Science in Aerospace Engineering at Delft University of Technology, November 10, 2011.

[11] M. J. Lighthill: Sound generated aerodynamically. Proc. Roy. Soc. A. **252** (1962) 147–182.

[12] O. M. Phillips: On the generation of sound by supersonic turbulent shear layers. J. Fluid Mech. **9** (1960) 1–28.

[13] J. E. Ffowcs Williams, A. J. Kempton: The noise from the large-scale structure of a jet. J. Fluid Mech. **84** (1978) 673–694.

[14] G. M. Lilley: On the noise from jet. AGARD CP **131** (1974) 1–12.

[15] F. L. Pan, A. Uzun, A. S. Lyrintzis: Refraction corrections for surface integral methods in jet aero acoustics. AIAA paper, AIAA-2004-2873, 2004.

[16] F. L. Pan, A. Uzun, A. S. Lyrintzis: Surface integral methods in jet aero acoustics: Refraction corrections. Journal of Aircraft **45** (2008) 381–387.

[17] J. H. E. Plumblee: Effects of forward velocity on turbulent jet mixing noise. Lockheed Missiles and Space Co. Report NASA CR-2702, 1976.

[18] J. Sanford: Acoustic refraction: A three-dimensional shear layer correction for microphone measurements in an open-jet acoustic wind tunnel. Journal of Undergraduate Research, University of Florida **10** (2008) 1–12.

[19] C. L. Morfey, P. F. Joseph: Shear layer refraction corrections for off-axis sources in a jet flow. Journal of Sound and Vibration **239** (2000) 819–984.

[20] A. Lauterbach, K. Ehrenfried, S. Kröber: Microphone array measurements on high-speed trains in wind tunnels. Berlin Beamforming Conference, 2010.

[21] L. Cattafesta, C. Bahr, N. Zawodny, T. Yardibi: Shear layer time-delay correction using a non-intrusive acoustic point source. Aero acoustics **10** (2011) 497–530.

[22] T. F. Brooks, W. M. Humphreys: A deconvolution approach for the mapping of acoustic sources (DAMAS) determined from phased microphone arrays. Journal of Sound and Vibration **294** (2006) 856–879.

[23] D. Döbler, R. Schröder, E. V. GFaI: Contrast improvement and sound reconstruction of quiet sound sources using a high dynamic range algorithm. Volmerstrasse 3, 12489 Berlin, Germany, BeBeC-2012-12, 2012.